

Theoretical Study of Isoelectronic Molecules: B₆H₁₀, 2-CB₅H₉, 2,3-C₂B₄H₈, 2,3,4-C₃B₃H₇, and 2,3,4,5-C₄B₂H₆

Shan Xi Tian

Hefei National Laboratory for Physical Sciences at Microscale, Laboratory of Bond Selective Chemistry, Department of Chemical Physics, University of Science and Technology of China, Hefei, Anhui 230026, People's Republic of China

Received: April 1, 2005; In Final Form: June 2, 2005

Isoelectronic molecules regarding B₆H₁₀, 2-CB₅H₉, 2,3-C₂B₄H₈, 2,3,4-C₃B₃H₇, and 2,3,4,5-C₄B₂H₆ are studied by the density functional B3LYP/6-311G(d,p) method and the electron propagator theory in the partial third-order quasiparticle approximation, as well as the extrapolated calculation with the coupled-cluster CCSD(T) theory. The calculated ionization potentials are in good agreement with the experimental data from photoelectron spectroscopy. Valence structures are characterized with natural orbital bond (NBO) theory, exhibiting the multiple three-center two-electron bonds B–H–B, B–B–B, C–B–B, B–C–B, and C–B–C, and chemical bond rearrangements in the cations.

1. Introduction

Boron hydrides, as the typical electron-deficient molecules, are extensively applied in chemistry. Studies of the geometrical and valence structures can provide impetus for discoveries of new species and reactions.¹ On the other hand, carboranes were discovered in the hunt for high-energy fuels during the early to middle 1950s.² Geometrical structures of carboranes are similar to boron hydrides, namely some boron atoms in the polyhedral boranes are replaced with carbon atoms. There are three main classes of carboranes: *closo*-C_{0–2}B_nH_{n+2}, *nido*-C_{0–4}B_nH_{n+4}, and *arachno*-C_{0–6}B_nH_{n+6}. The structures of the *nido*- and *arachno*-carboranes are constructed by sequentially leaving unoccupied one and two vertexes respectively from the various *closo*-deltahedra. In the boranes and carboranes, the hydrogen atoms may locate at the terminal positions of the polyhedral skeleton (noted as H_t) or connected with two boron or one carbon and one boron atoms (noted as the bridging hydrogen, H_b). The latter, X–H_b–Y (X, Y = B, C), exhibits a three-center two-electron (3c-2e) bond. The B–H_b–B bond is most energetically favorable,³ although the B–H_b–C bonds was found in *nido*-2,3,5-C₃B₃H₇^{4a} and *nido*-2,4-C₂B₄H₈.^{4b}

As far as hexaborane(10), B₆H₁₀, it is an especially interesting molecule from the point of view of reactivity, since it has four nonequivalent borons at which reaction may occur. This molecule is fluxional at room temperature, due to a rapid tautomerization of the H_b atoms.⁵ Four neutral carborane derivatives of B₆H₁₀, namely its isoelectronic molecules 2-CB₅H₉, 2,3-C₂B₄H₈, 2,3,4-C₃B₃H₇, and 2,3,4,5-C₄B₂H₆, have been prepared and characterized.⁶ In these molecules, carbon atoms prefer two-center bonding while boron atoms are more likely to participate in three-center bonds. These five isoelectronic molecules were recently proved to be the most stable isomers at the MP2/6-31G* level of theory.³ The calculated B¹¹ chemical shifts for these species were also in good agreement with the experimental data.⁷ On the other hand, difficulties in elucidating the valence structures were met in the localized orbital analysis.⁸ Multiple bonding in these isoelectronic molecules leads to suspicions of various valence structures.⁸ A reasonable ab initio study and the localized natural bond orbital (NBO)⁹ analysis

are necessary for insights into their valence structures. Moreover, the reassignments to their photoelectron spectra are required, because the previous assignments were made on the basis of the low-level self-consistent field (SCF) calculations and Koopmans' theorem.¹⁰

The NBO analysis transfers the delocalized molecular orbitals into the localized ones that are closely tied to chemical bond concepts. Filled NBOs describe the hypothetical, strictly localized Lewis structure.⁹ NBO theory is powerful to describe the multiple bonds in the carboranes. To derive the accurate vertical ionization potentials (IP_v), electron correlation and orbital relaxation effects should be considered. Thereby, the efficient partial third-order quasiparticle theory (P3) developed by Ortiz et al.¹¹ is applied in this work. In the quasiparticle approximation, electrons assigned to canonical MOs are subject to a correlated, energy-dependent potential represented by the diagonal elements of the self-energy matrix while nondiagonal elements are neglected.¹¹ Each IP_v calculated with the electron propagator method corresponds to a Dyson orbital, and pole strength is equal to the integral over all space of the absolute value squared of the Dyson orbital, indicating the perturbation to the results of Koopmans' theorem.¹¹ Validity of the P3 theory has been demonstrated in the prediction of the IP_v values for boron hydrides in our recent work.¹² B₆H₁₀ and its isoelectronic molecules 2-CB₅H₉, 2,3-C₂B₄H₈, 2,3,4-C₃B₃H₇, and 2,3,4,5-C₄B₂H₆ will be studied in this work. The geometrical, vibrational, and energetic properties, the IP_v, and the adiabatic IP (IP_a) values will be compared with the experimental data.¹⁰ NBO analysis will be performed on the basis of the calculated wave functions of molecular orbitals (MOs). This theoretical study may aid in the assignments of the spectra measured with a higher energy resolution and a good understanding of the valence characteristics of carboranes.

2. Calculation Details

The geometrical parameters of each neutral species at C_s symmetry and its cation were fully optimized by the hybrid density functional B3LYP method. Harmonic vibrational frequencies were determined analytically. The single and double

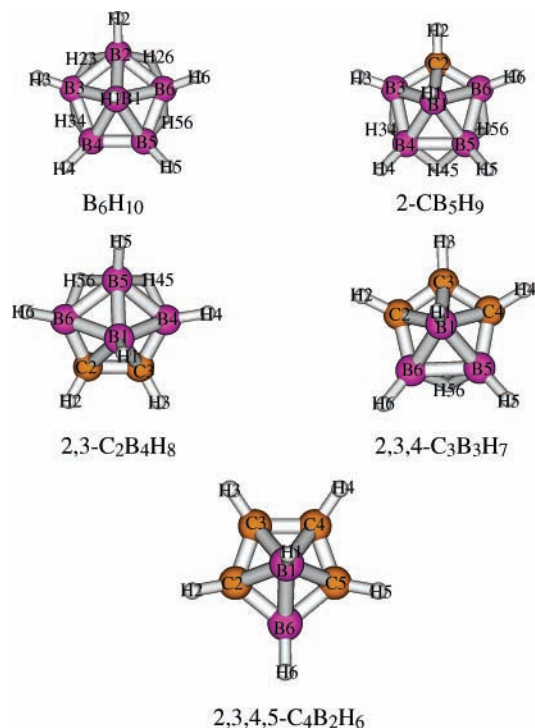


Figure 1. Molecular structures of B_6H_{10} , $2-CB_5H_9$, $2,3-C_2B_4H_8$, $2,3,4-C_3B_3H_7$, and $2,3,4,5-C_4B_2H_6$.

excitation coupled-cluster theory including a perturbative estimate of triple excitations (CCSD(T))¹³ was applied in the extrapolated energetic calculations over the B3LYP optimized geometries to obtain the atomization energies of the neutral species (with respect to H^2S and B^2P) and the IP_a values. The IP_v values were predicted by using the P3 approximation of the electron propagator theory. As pointed out before, the polarization functions on hydrogen atoms improved the description of the bridging hydrogen atoms in carboranes.^{12,14} Thereby, the 6-311G(d,p) basis set was used throughout the calculations. The B3LYP wave functions were used for NBO analysis, and a three-center bond search was activated by the keyword 3CBOND.¹⁵ Ab initio calculations were performed with Gaussian 98.¹⁶

Molecular maps were produced by the MOLDEN graphics program.¹⁷ The contour values in the MO electron density plots are equal to ± 0.05 .

3. Results and Discussion

The molecular structures are shown in Figure 1. The density contour maps of the frontier MOs of each species are shown in Figure 2. Correlation between the number of carbon or H_b atoms in carboranes and the atomization energy is shown in Figure 3. Figure 4 shows a comparison between the calculated IP_v and the experimental PES from ref 10. Valence structures for the stable neutral and radical cations are given in Figure 5 on the basis of NBO analyses. The calculated geometrical parameters, atomization energies, and IP values are listed in Tables 1–7. Natural atomic populations (NAP) are listed in Table 8 for both the neutral and radical cations. Occupancies and energetic levels of the 3c-2e bonds in the neutral are given in Table 9.

3.1. Geometrical Structures and Harmonic Vibrational Frequencies. The structures of the neutral species of present interest are shown in Figure 1, in which the connections or bonds between two atoms are illustrated automatically by MOLDEN program and do not mean the real chemical bonds. Ionization

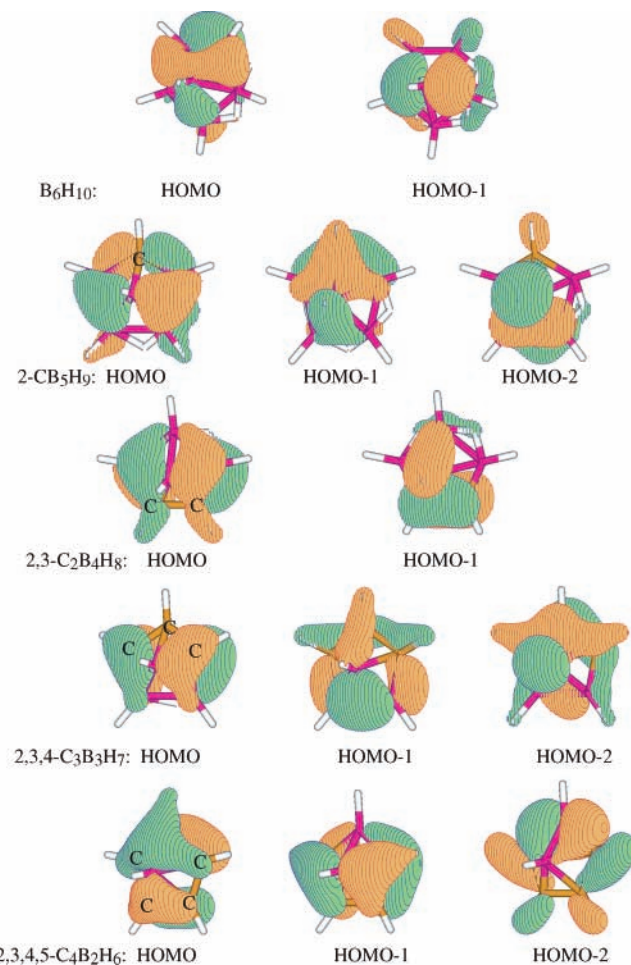


Figure 2. Electron density maps of HOMO, HOMO-1, and HOMO-2.

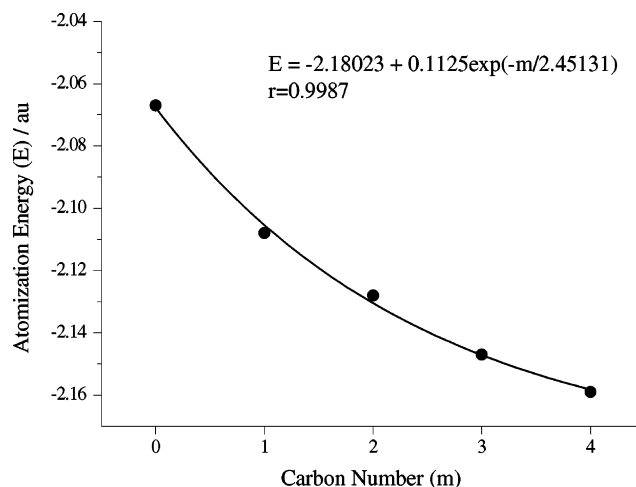


Figure 3. Correlation between atomization energy (calculated at the CCSD(T)/6-311G(d,p)//B3LYP/6-311G(d,p) level) and carbon number of carboranes.

slightly changes the geometrical parameters of the neutral (see the Cartesian geometries in the Supporting Information), thereby no diagrams of the radical cations are shown. In Table 1, the experimental data of the geometries¹⁸ and the MP2/6-31G* calculated results⁷ are compared with the present predictions. In general, the distances between two heavy atoms and heavy atom– H_b predicted at the B3LYP/6-311G(d,p) level are a little longer than those calculated at the MP2/6-31G* level. The

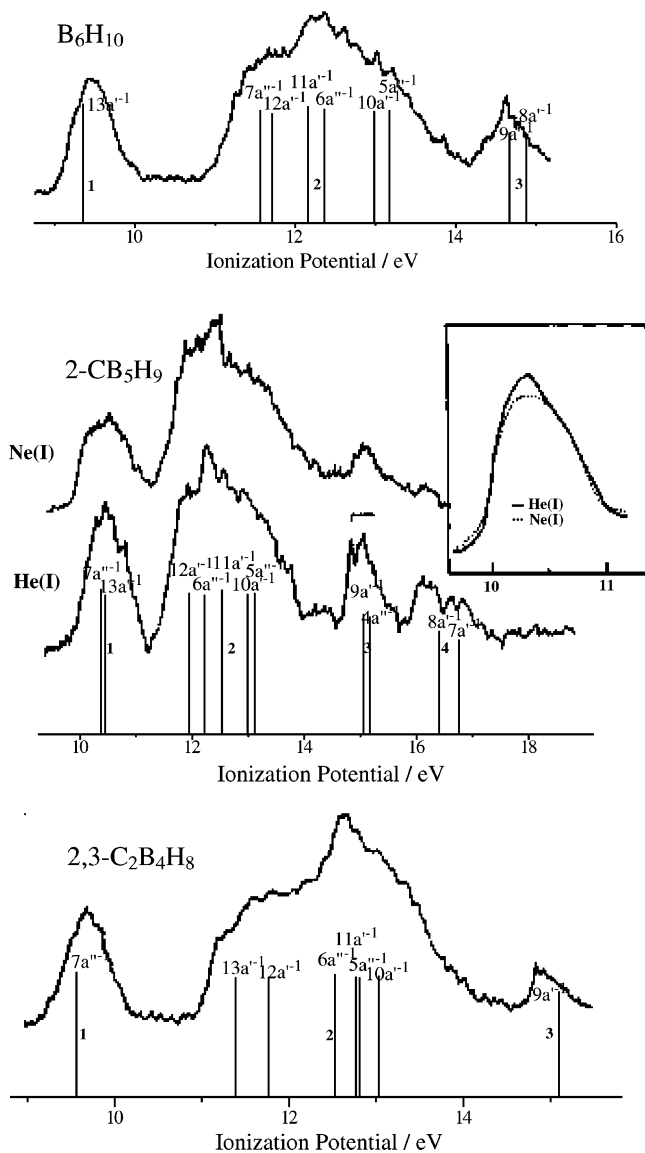


Figure 4. Reassignments to the photoelectron spectra adopted from ref 10, with the copyright permission from the American Chemical Society.

experimental data distinctly differ from the theoretical predictions, due to the crystal electrostatic field in the solids.

As far as B_6H_{10} and its cation, the longest distance (1.818 Å) is between B1 and B4(5) in the neutral, while it is shortened to 1.760 Å in the cation. The other shortened distance is between B2 and B3(6). However, the distances of B1B2, B1B3(6), B3(6)B4(5), B4B5 in the neutral are elongated after ionization relaxation. Such changes can be observed for the other species. The most significant elongation of the bond distance due to ionization is 0.151 Å of B4B5 in B_6H_{10} , 0.140 Å of B1B3(6) in 2- CB_5H_9 , 0.118 Å of B5B6(4) in 2,3- $C_2B_4H_8$, and 0.076 Å of B1C3(4) in 2,3,4,5- $C_4B_2H_6$, respectively, while the most significantly shortened bond distances are -0.058 Å of B1B4(5) in B_6H_{10} , -0.101 Å of B1C2 in 2- CB_5H_9 , -0.047 Å of C2C3 in 2,3- $C_2B_4H_8$, and -0.032 Å of C2(4)C3(5) in 2,3,4,5- $C_4B_2H_6$, respectively. The C_s symmetry of 2,3,4- $C_3B_3H_7$ is distorted by ionization—two significantly unequal bond distances are predicted for B1C2 and B1C4, B1B6 and B1B5, C2C3 and C3C4, and C2B6 and C4B5, as well as for the heavy atom– H_b distances.

Harmonic vibrational frequencies listed in Table 1S in the Supporting Information show that there are red shifts from the

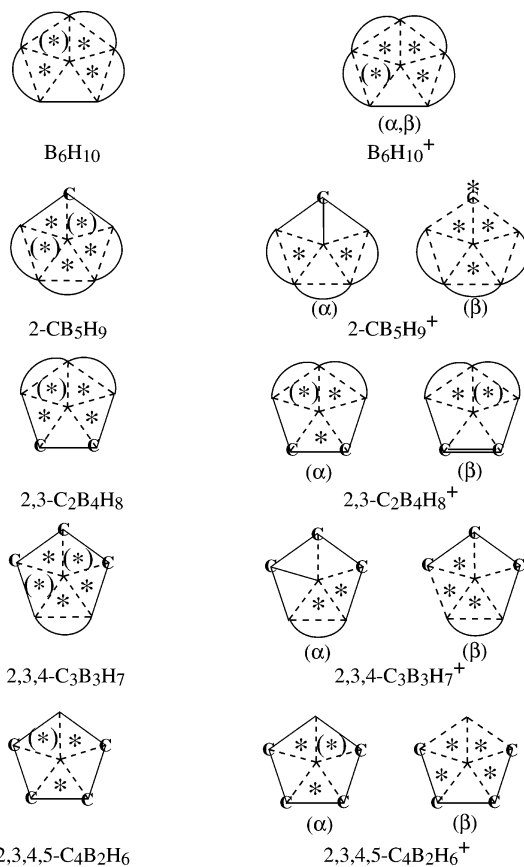


Figure 5. Schemes of valence structures of the neutral and cations. An asterisk represents the three-center bonds involving the heavy atoms (an asterisk in parenthesis exhibits the valence resonance due to C_s symmetry); curves represent the B–H–B bonds; lines represent conventional covalent bonds; double lines represent a degenerate bond.

neutral to the cations for the lower frequencies (<1000 cm^{-1}) while there are blue shifts for the higher frequencies. The lower frequencies correspond to the vibrations of the molecular polyhedra (heavy atoms), while the higher frequencies correspond to the stretching or wagging vibrations of the C– H_t , B– H_t , or H_b atoms.

3.2. Energetic Analyses and Assignments to the PES. The calculated atomization energies of the neutral carboranes are compared with the experimental data in Table 2. Only one experimental value, -2.091 au of B_6H_{10} , is available;¹⁹ the CCSD(T) prediction -2.067 au is close to this value. Both the B3LYP and CCSD(T) results demonstrate that the absolute values of atomization energy increase with the increase of the number (m) of carbon atoms in carboranes. Correlation between the atomization energy and m is plotted in Figure 3 and fitted with an exponential function, atomization energy = $-2.18023 + 0.1125 \exp(-m/2.45131)$. On the other hand, this correlation also can be between the atomization energy and the number (n) of H_b atoms in carboranes, atomization energy = $-3.10308 + 0.91405 \exp(n/31.728)$ with a correlation rate $r = 0.9995$. To rationalize the thermodynamic stability, a linear function, atomization energy = $-0.5168n + -0.5475m$, has been obtained. Namely, suppose one 3c-2e B– H_b –B bond energy is ca. -0.03 au, a replacement of a B–B bond with a B–C bond stabilizes the species by ca. -0.06 au.²⁰

He(I) and Ne(I) PES of B_6H_{10} , 2- CB_5H_9 , and 2,3- $C_2B_4H_8$ were reported by Ulman and Fehlner, in which three, four, and three diffuse bands were observed, respectively, in the He(I) energy range.¹⁰ Their assignments were made on the basis of the SCF orbital energy calculations^{8,21} and the ring-polar

TABLE 1: Geometrical Parameters for the Neutral and Cations (Bond Lengths in Å)

	B1B2	B1B3	B1B4	B2B3	B3B4	B4B5	B2H23	B3H23	B3H34	B4H34
B₆H₁₀ (C_s)										
B3LYP/6-311G(d,p)	1.748	1.757	1.818	1.801	1.742	1.636	1.297	1.378	1.328	1.336
MP2/6-31G* ^a	1.741	1.748	1.800	1.782	1.732	1.638	1.298	1.369	1.327	1.329
exptl (X-ray) ^b	1.736	1.753	1.795	1.794	1.737	1.596	1.32	1.48	1.31	1.35
exptl (MW) ^c	1.774	1.762	1.783	1.818	1.710	1.654				
B₆H₁₀⁺ (C_s)										
B3LYP/6-311G(d,p)	1.771	1.796	1.760	1.779	1.747	1.787	1.325	1.333	1.323	1.342
	B1C2	B1B3	B1B4	C2B3	B3B4	B4B5	B3H34	B4H34	B4H45	
2-CB₅H₉ (C_s)										
B3LYP/6-311G(d,p)	1.747	1.811	1.746	1.507	1.775	1.818	1.364	1.301	1.330	
MP2/6-31G* ^a	1.731	1.791	1.738	1.511	1.757	1.797	1.352	1.303	1.327	
exptl (partial MW) ^d		1.782	1.781		1.759	1.830				
2-CB₅H₉⁺ (C_s)										
B3LYP/6-311G(d,p)	1.646	1.951	1.816	1.519	1.901	1.735	1.344	1.309	1.323	
	B1C2	B1B4	B1B5	C2C3	C2B6	B5B6	B5H56	B6H56		
2,3-C₂B₄H₈ (C_s)										
B3LYP/6-311G(d,p)	1.763	1.790	1.725	1.422	1.518	1.792	1.317	1.336		
MP2/6-31G* ^a	1.737	1.773	1.722	1.426	1.520	1.773	1.334	1.312		
exptl ^e	1.750	1.772	1.715	1.418	1.499	1.790	1.308	1.280		
2,3-C₂B₄H₈⁺ (C_s)										
B3LYP/6-311G(d,p)	1.757	1.831	1.799	1.375	1.580	1.810	1.329	1.316		
	B1C3	B1C2	B1B6	C2C3	C2B6	B5B6	B5H56			
2,3,4-C₃B₃H₇ (C_s)										
B3LYP/6-311G(d,p)	1.755	1.735	1.766	1.425	1.533	1.780	1.323			
MP2/6-31G* ^a	1.729	1.718	1.754	1.426	1.532	1.760	1.319			
2,3,4-C₃B₃H₇⁺ (C₁)										
B3LYP/6-311G(d,p)	1.842	1.829	1.827	1.429	1.540	1.745	1.313			
		1.666	1.736	1.398	1.711		1.329			
	B1C3	B1C2	B1B6	C3C4	C2C3	C2B6				
2,3,4,5-C₄B₂H₆ (C_s)										
B3LYP/6-311G(d,p)		1.717	1.715	1.845	1.422	1.442	1.530			
MP2/6-31G* ^a		1.701	1.701	1.821	1.424	1.439	1.528			
exptl (MW) ^f		1.697	1.709	1.886	1.424	1.436	1.541			
2,3,4,5-C₄B₂H₆⁺ (C_s)										
B3LYP/6-311G(d,p)		1.793	1.695	1.864	1.458	1.410	1.577			

^a From ref 7. ^b X-ray data from ref 18a. ^c Microwave spectra from ref 18b. ^d No carbon positions were refined in ref 18c. ^e From ref 18d. ^f Microwave spectra from ref 18e.

TABLE 2: Atomization Energies (in au) of the Neutral Carboranes in Comparison with Experimental Data

	B3LYP ^a	CCSD(T)	exptl
B ₆ H ₁₀	-2.161 (-2.042)	-2.067	-2.091 ^b
2-CB ₅ H ₉	-2.210 (-2.097)	-2.108	
2,3-C ₂ B ₄ H ₈	-2.235 (-2.129)	-2.127	
2,3,4-C ₃ B ₃ H ₇	-2.262 (-2.162)	-2.147	
2,3,4,5-C ₄ B ₂ H ₆	-2.281 (-2.188)	-2.159	

^a The values in parentheses are corrected with the zero-point vibrational energies. ^b From ref 19.

model.^{10,21} The weakness and roughness of the ring-polar model are known,²² therefore it is only a convenient tool for discussing the spectra qualitatively. To reassign these spectra, the P3 calculations are performed over the B3LYP/6-311G(d,p) optimized geometries of the neutral. The calculated IP_v values of the outer valence orbitals are compared with the experimental data¹⁰ for B₆H₁₀, 2-CB₅H₉, and 2,3-C₂B₄H₈ in Tables 4, 5, and 6, respectively. The calculated results are in good agreement with the experimental data. In Figure 4, the experimental spectra are adopted from ref 10 and reassigned on the basis of the present P3 calculations.

The previous SCF Koopmans' assignments¹⁰ qualitatively agree with the present assignments to the spectrum of B₆H₁₀, namely one ionization state corresponds to the first band, and

TABLE 3: Vertical Ionization Potentials (IP_v in eV) and Pole Strengths (in Parentheses) of B₆H₁₀ in Comparison with the Experimental Data

orbital assign	theorl IP _v	exptl IP _v ^a
13a'	9.349 (0.90)	9.4
7a''	11.565 (0.89)	11.6
12a'	11.712 (0.89)	
11a'	12.157 (0.90)	
6a''	12.362 (0.89)	12.2
10a'	12.979 (0.89)	
5a''	13.168 (0.89)	
9a'	14.664 (0.87)	14.6
8a'	14.875 (0.86)	
4a''	16.123 (0.83)	
7a'	16.643 (0.79)	
6a'	19.281 (0.79)	

^a From He(I) PES of ref 10.

four and two states are for the next two bands, respectively. In particular, 7a''⁻¹ and 12a'⁻¹ lead to the flat front shoulder, 11a'⁻¹ and 6a''⁻¹ correspond to the middle peaks, and 10a'⁻¹ and 5a''⁻¹ are at the rear shoulder of the second band, respectively. Two states, 7a''⁻¹ and 13a'⁻¹, lead to the first band in the spectra of 2-CB₅H₉, and it is noted that the ring-polar model successfully predicted this assignment.¹⁰ However, the ring-polar model failed in the assignments for the next two bands, namely, three states were suspected for the third band and one state for the

TABLE 4: Vertical Ionization Potentials (IP_v in eV) and Pole Strengths (in Parentheses) of 2-CB₅H₉ in Comparison with the Experimental Data

orbital assign	theor IP _v	exptl IP _v ^a
7a''	10.374 (0.90)	}10.5
13a'	10.449 (0.89)	
12a'	11.944 (0.90)	11.8
6a''	12.220 (0.89)	12.2
11a'	12.530 (0.90)	12.4
10a'	12.990 (0.89)	
5a''	13.113 (0.90)	
9a'	15.051 (0.87)	(14.7)
4a''	15.171 (0.86)	14.9
8a'	16.402 (0.85)	16.1
7a'	16.753 (0.84)	16.6
3a''	19.556 (0.82)	

^a From He(I) PES of ref 10.**TABLE 5: Vertical Ionization Potentials (IP_v in eV) and Pole Strengths (in Parentheses) of 2,3-C₂B₄H₈ in Comparison with the Experimental Data**

orbital assign	theor IP _v	exptl IP _v ^a
7a''	9.564 (0.90)	9.6
13a'	11.386 (0.89)	11.3
12a'	11.765 (0.89)	11.7
6a''	12.526 (0.90)	12.3
11a'	12.767 (0.89)	
5a''	12.810 (0.89)	
10a'	13.030 (0.90)	
9a'	15.098 (0.86)	14.9
8a'	15.740 (0.85)	
4a''	16.952 (0.85)	
7a'	17.132 (0.84)	
3a''	19.746 (0.81)	

^a From He(I) PES of ref 10.**TABLE 6: Vertical Ionization Potentials (IP_v in eV) and Pole Strengths (in Parentheses) of 2,3,4-C₃B₃H₇ and 2,3,4,5-C₄B₂H₆**

2,3,4-C ₃ B ₃ H ₇		2,3,4,5-C ₄ B ₂ H ₆	
orbital assign	theor IP _v	orbital assign	theor IP _v
7a''	9.959 (0.90)	13a'	9.315 (0.91)
13a'	10.211 (0.90)	7a''	10.525 (0.90)
12a'	11.943 (0.89)	6a''	11.669 (0.90)
6a''	12.411 (0.90)	12a'	12.153 (0.90)
11a'	12.606 (0.90)	11a'	12.450 (0.89)
10a'	13.012 (0.90)	10a'	13.807 (0.89)
5a''	13.963 (0.89)	5a''	14.229 (0.89)
4a''	15.589 (0.86)	9a'	15.859 (0.85)
9a'	15.832 (0.84)	8a'	15.959 (0.84)
8a'	17.218 (0.86)	4a''	17.804 (0.86)
7a'	17.667 (0.86)	7a'	17.991 (0.86)

forth band.¹⁰ The P3 results indicate that there are two states for each one of the last two bands, in reasonable agreement with two experimental peaks for each band (see Figure 4). As for the spectrum of 2,3-C₂B₄H₈, two states (13a⁻¹ and 12a⁻¹) correspond to the flat shoulder of the second diffuse band and four states, 6a⁻¹, 11a⁻¹, 5a⁻¹, and 10a⁻¹, swarm to form the high peaks of the second band. No experimental spectra of 2,3,4-C₃B₃H₇ and 2,3,4,5-C₄B₂H₆ are available; the theoretical IP_v values for these two species are listed in Table 7. Here some comments on the present P3 calculations should be addressed. Although the P3 calculations succeed in predicting the IP_v for the outer valence orbitals of the numerous molecules,^{11b,12} the predictions are poor for the ionization processes where the single-electron rule is broken. Strong electron configuration interactions should be included to predict the satellites in the PES. The IP_v values of the inner orbitals (for example, 4a'',

TABLE 7: The Lowest Adiabatic Ionization Potentials (IP_a in eV) of the Neutral Carboranes in Comparison with the Experimental Data

	B ₆ H ₁₀	2-CB ₅ H ₉	2,3-C ₂ B ₄ H ₈	2,3,4-C ₃ B ₃ H ₇	2,3,4,5-C ₄ B ₂ H ₆
theor ^a	8.849 (8.804)	9.697 (9.600)	9.302 (9.221)	9.587 (9.480)	8.907 (8.849)
exptl	9.0 ^b	~9.7 ^c	~9.3 ^c	9.548	8.882

^a From the top to the bottom, they are the results calculated at the B3LYP/6-311G(d,p) level, those including the zero-point vibration energy corrections (in parentheses), and those at the CCSD(T)/6-311G(d,p)//B3LYP/6-311G(d,p) level, respectively. ^b From He(I) PES of ref 10. ^c Estimated from PES in ref 10.

TABLE 8: Natural Atomic Population Charges of the Neutral and Cationic Carboranes

	neutral	cation	neutral	cation
B ₆ H ₁₀			2-CB ₅ H ₉	
B1	-0.24527	-0.31606	B1	-0.07575
B2	-0.18155	-0.06023	C2	-0.70849
B3	-0.05796	-0.07895	B3	0.12621
B4	-0.15527	0.15150	B4	-0.15732
H1	0.06699	0.13672	H1	0.04301
H2	0.06673	0.10875	H2	0.25272
H3	0.04671	0.11034	H3	0.01693
H4	0.03477	0.06338	H4	0.05764
H23	0.14569	0.17500	H34	0.12647
H34	0.13262	0.14413	H45	0.14865
2,3-C ₂ B ₄ H ₈			2,3,4-C ₃ B ₃ H ₇	
B1	0.05608	0.20278	B1	0.18618
C2	-0.39938	-0.33910	C2	-0.44770
B5	-0.13702	-0.13790	(C4) ^a	-0.28585
B6	0.00759	0.24223	C3	-0.15976
H1	0.02798	0.05114	B5	-0.01064
H2	0.23250	0.29427	(B6) ^a	0.02349
H5	0.05079	0.10061	H1	0.01517
H6	0.02721	0.05481	H2	0.28860
H56	0.13316	0.13947	(H4) ^a	0.23740
			H3	0.22672
			H5	0.02324
			(H6) ^a	0.08368
			H56	0.12708
2,3,4,5-C ₄ B ₂ H ₆				0.13776
B1	0.29827	0.42614		
C2	-0.49791	-0.45417		
C3	-0.21414	-0.10398		
B6	0.20424	0.46700		
H1	0.00341	0.05264		
H2	0.23336	0.28786		
H3	0.23261	0.27617		
H6	-0.01378	0.04248		

^a Due to C₁ symmetry of 2,3,4-C₃B₃H₇⁺.

7a', and 6a' of B₆H₁₀, see Table 4) exhibit the smaller pole strengths, indicating that the P3 approximation may be invalid for these ionization states. Moreover, the rear shoulder (at ca. 14 eV) of the second band for B₆H₁₀, the small peak around 14.2 eV in the He(I) spectrum of 2-CB₅H₉, and the rear shoulder (at ca. 13.5 eV) of the second band for 2,3-C₂B₄H₈ suggest that the shake-up or shake-off satellites may appear. On the basis of the optimized structures of both the neutral and cations, we obtain the lowest IP_a values and compare them with the experimental data.¹⁰ The experimental IP_a values of 2-CB₅H₉ and 2,3-C₂B₄H₈ are estimated from the spectra.¹⁰ In Table 8, one can find that the theoretical data match the experimental IP_a values well.

To elucidate the different split energies between the first two ionization states for B₆H₁₀, 2-CB₅H₉, and 2,3-C₂B₄H₈, the ring-polar model suggested that it was due to the interactions between ring and polar p components.¹⁰ Electron density maps of the

highest occupied MO (HOMO), the next HOMO (HOMO-1), and the third HOMO (HOMO-2) in Figure 2 show the bond characteristics. Namely, the interaction between B1 p_x and two bridging H34 and H56 atoms (HOMO) is comparable to that between B1 p_y and C2 p_z (HOMO-1) in 2-CB₅H₉, which is the same as the explanation using the ring-polar model.¹⁰ However, the interaction between B1 p_x and four bridging H23, H34, H45, and H56 atoms is much stronger than that between B1 p_y and two p_z components of B4 and B5 in B₆H₁₀—the former leads to the lower HOMO-1 while the latter leads to the higher HOMO. This situation reverses the energy levels for 2,3-C₂B₄H₈, namely the stronger B1 p_y and two p_z components of the C2 and C3 (pseudo- π) interaction leads to the lower HOMO-1. Similar interactions lead to the energetically close HOMO and HOMO-1 of 2,3,4-C₃B₃H₇ but equivalent split energies among HOMO, HOMO-1, and HOMO-2 of 2,3,4,5-C₄B₂H₆.

3.3. NAP Charge Analyses and Valence Structures. The NAP charges of the neutral and cations are presented in Table 8 on the basis of the NBO analyses. It is interesting that the NAP charge on the B1 atom increases from the negative to the positive when the carbon number in the carborane increases. The B atoms near the C atoms on the penta-ring have the positive (or less negative) NAP charge. Epstein et al. tried to explain the asymmetric B–H_b–B bridges of B₆H₁₀ through the Mulliken charge analyses, namely, the bridging H atom lay to the more negative (or less positive) B atoms.⁸ It may be true for the H23(26) atom in B₆H₁₀. The B2H23 bond (1.297 Å) is shorter than the B3H23 bond (1.378 Å), which is somehow due to the more negative NAP charge on B2 (−0.18155) with respect to B3 (−0.05796). In contrast to the H23(26) atom, the B3H34 bond (1.328 Å) is slightly shorter than the B4H34 bond (1.336 Å), while the NAP charge on the B4 atom (−0.15527) is much more negative than that on the B3 atom. The above NAP charge analyses indicate that the localized electrostatic interaction is not the only reason of the asymmetric B–H_b–B bridges.

The existence of a number of equivalent valence structures consistent with a given molecular configuration is one of the most interesting and ambiguous aspects of boron chemistry. B₆H₁₀ may have 12 possible 3c-2e valence structures.⁸ Here the results concluded by Epstein et al. are recalled. Two three-center bonds involving only B atoms were proposed in the most stable B₆H₁₀ and 2-CB₅H₉: 2,3-C₂B₄H₈ and 2,3,4-C₃B₃H₇ preferred two resonance structures, respectively; 2,3,4,5-C₄B₂H₆ might be one of three preferable structures.⁸ The present NBO analyses show the most possible valence structures of the neutral and cations in Figure 5, and occupancies and energetic levels of the 3c-2e bonds such as B–B–B, B–H–B, C–B–B, and C–B–C are summarized in Table 9. As shown in Figure 5, three three-center bonds besides the B–H–B bond exist in B₆H₁₀, 2-CB₅H₉, 2,3-C₂B₄H₈, and 2,3,4-C₃B₃H₇, while two three-center bonds, C–B–B and C–B–C, exist in 2,3,4,5-C₄B₂H₆, which is similar to the structures in columns 1 and 3 of Table 11 in ref 8. The valence structures of the neutral reform remarkably after ionization. One three-center bond is changed from B3–B1–B4 to B2–B1–B3 for B₆H₁₀⁺. Different electron spins (α and β) show the distinct valence structures for the other cations. In particular, the open three-center bond B–C–B is shown in 2-CB₅H₉⁺(β); the double C–C bond is shown in 2,3-C₂B₄H₈⁺(β); the multiple three-center bonds are shown in 2,3,4,5-C₄B₂H₆⁺(β). The occupancies of B2–B1–B6 and B5–B1–B6 in B₆H₁₀, B4–B1–B5 and B5–B1–B6 in 2-CB₅H₉, C3–B1–B4 and B4–B1–B5 in 2,3-C₂B₄H₈, and C4–B1–B5 and B5–B1–B6 in 2,3,4-C₃B₃H₇ are smaller and the energy levels are higher. This indicates that these bonds are relatively

TABLE 9: Occupancy and Energy (au) of the Three-Center Two-Electron (3c-2e) Bonds of the Neutral Carboranes

	3c-2e bond	occupancy	energy
B ₆ H ₁₀	B2–B1–B6	1.67193	−0.39736
	B3–B1–B4	1.85172	−0.52233
	B5–B1–B6	1.62851	−0.33622
	B2–H23–B3	1.97879	−0.58162
	B2–H26–B6	1.90638	−0.49412
	B3–H34–B4	1.96394	−0.53306
2-CB ₅ H ₉	B5–H56–B6	1.90738	−0.49095
	C2–B1–B3	1.80315	−0.47752
	B4–B1–B5	1.65181	−0.39931
	B5–B1–B6	1.58809	−0.31219
	B3–H34–B4	1.98018	−0.57062
	B4–H45–B5	1.90911	−0.49541
2,3-C ₂ B ₄ H ₈	B5–H56–B6	1.91624	−0.50098
	C2–B1–B6	1.79837	−0.46939
	C3–B1–B4	1.62399	−0.34222
	B4–B1–B5	1.65123	−0.36858
	B4–H45–B5	1.97800	−0.56452
	B5–H56–B6	1.90351	−0.47770
2,3,4-C ₃ B ₃ H ₇	C2–B1–C3	1.89024	−0.51213
	C4–B1–B5	1.64955	−0.37217
	B5–B1–B6	1.60861	−0.29911
	B5–H56–B6	1.89744	−0.46315
2,3,4,5-C ₄ B ₂ H ₆	C2–B1–B6	1.82273	−0.44931
	C3–B1–C4	1.91556	−0.52373

weaker and may correlate with valence resonances. Namely, the structures in Figure 5 only represent the lowest energetic ones, the higher or excited states may show the different valence structures possible shown in ref 8. The hybrids of the three-center bonds are given as Table 2S in the Supporting Information.

4. Conclusion

Geometries, vibrational frequencies, and energetic properties of B₆H₁₀, 2-CB₅H₉, 2,3-C₂B₄H₈, 2,3,4-C₃B₃H₇, and 2,3,4,5-C₄B₂H₆, and their radical cations, are studied with B3LYP/6-311G(d,p), CCSD(T), and the P3 calculations. Atomization energies of these species are enhanced in an exponential term of the carbon number in the carboranes, owing to the strong B–C bond formation. The predicted IP_v values are used to make reassignments to the PES available in the literature.¹⁰ Valence structures are presented on the basis of the NBO analyses, exhibiting the multiple three-center bonds such as B–B–B, B–H–B, C–B–B, and C–B–C. In the cations, the valence structures are rearranged and distinctly differ from those of the neutral.

Supporting Information Available: Cartesian coordinates of the neutral and cations, harmonic vibrational frequencies, and hybrids of the three-center bonds. This material is available free of charge via the Internet at <http://pubs.acs.org>.

References and Notes

- (1) (a) Lipscomb, W. N. *Boron Hydrides*; W. A. Benjamin, Inc.: New York, 1963. (b) Shore, S. G. *Boron Hydride Chemistry*; Muettterties, E. L., Ed.; Academic Press: New York, 1975. (c) Onak, T. *Comprehensive Organometallic Chemistry*; Wilkinson, G., Stone, F. G. A., Abel, E., Eds.; Pergamon: Oxford, England, 1982.
- (2) Williams, R. E. *Adv. Inorg. Radiochem.* **1976**, *18*, 67.
- (3) Hofmann, M.; Fox, M. A.; Greatrex, R.; Schleyer, P. v. R.; Williams, R. E. *Inorg. Chem.* **2001**, *40*, 1790.
- (4) (a) Fessenbecker, A.; Hergel, A.; Hettrich, R.; Schafer, V.; Siebert, W. *Chem. Ber.* **1993**, *126*, 2205. (b) Wrackmeyer, B.; Schanz, H.-J.; Milius, W. *Angew. Chem., Int. Ed. Engl.* **1997**, *36*, 75.
- (5) (a) Brice, V. T.; Johnson, H. D., II; Shore, S. G. *J. Chem. Soc., Chem. Commun.* **1972**, 1128. (b) Brice, V. T.; Johnson, H. D., II; Shore, S. G. *J. Am. Chem. Soc.* **1973**, *95*, 6629.

- (6) (a) Onak, T. P.; Dunks, G. B.; Spielman, J. R.; Gerhart, F. J.; Williams, R. E. *J. Am. Chem. Soc.* **1966**, *88*, 2061. (b) Onak, T. P. *Inorg. Chem.* **1968**, *7*, 1043. (c) Bramlett, C. L.; Grimes, R. N. *J. Am. Chem. Soc.* **1966**, *88*, 4269.
- (7) Bühl, M.; Schleyer, P. v. R. *J. Am. Chem. Soc.* **1992**, *114*, 477.
- (8) Epstein, I. R.; Tossell, J. A.; Switke, E.; Stevens, R. M.; Lipscomb, W. N. *Inorg. Chem.* **1971**, *10*, 171.
- (9) Reed, A.; Curtiss, L. A.; Weinhold, F. *Chem. Rev.* **1988**, *88*, 899.
- (10) Ulman, J. A.; Fehner, T. P. *J. Am. Chem. Soc.* **1978**, *100*, 449.
- (11) (a) Ortiz, J. V. *J. Chem. Phys.* **1996**, *104*, 7599. (b) Ferreira, A. M.; Seabra, G.; Dolgounitcheva, O.; Zakrzewski, V. G.; Ortiz, J. V. In *Quantum-Mechanical Prediction of Thermochemical Data*; Cioslowski, J., Ed.; Kluwer: Dordrecht, The Netherlands, 2001; p 131.
- (12) Tian, S. X. *J. Phys. Chem. A* **2005**, *109*, 5471.
- (13) (a) Bartlett, R. J. *J. Phys. Chem.* **1989**, *93*, 1697. (b) Kucharski, S. A.; Bartlett, R. J. *Adv. Quantum Chem.* **1986**, *18*, 281. (c) Bartlett, R. J.; Stanton, J. F. In *Reviews of Computational Chemistry*; Lipkowitz, K. B., Boyd, D. B., Eds.; VCH Publishers: New York, 1995; Vol. V., Chapter 2, p 65.
- (14) Stanton, J. F.; Lipscomb, W. N.; Bartlett, R. J.; McKee, M. L. *Inorg. Chem.* **1989**, *28*, 109.
- (15) *NBO*, Version 3.1; Glendening, E. D., Reed, J. E., Carpenter, J. E., Weinhold, F.
- (16) Frisch, M. J.; Trucks, G. W.; Schlegel, H. B.; Scuseria, G. E.; Robb, M. A.; Cheeseman, J. R.; Zakrzewski, V. G.; Montgomery, J. A., Jr.; Stratmann, R. E.; Burant, J. C.; Dapprich, S.; Millam, J. M.; Daniels, A. D.; Kudin, K. N.; Strain, M. C.; Farkas, O.; Tomasi, J.; Barone, V.; Cossi, M.; Cammi, R.; Mennucci, B.; Pomelli, C.; Adamo, C.; Clifford, S.; Ochterski, J.; Petersson, G. A.; Ayala, P. Y.; Cui, Q.; Morokuma, K.; Malick, D. K.; Rabuck, A. D.; Raghavachari, K.; Foresman, J. B.; Cioslowski, J.; Ortiz, J. V.; Baboul, A. G.; Stefanov, B. B.; Liu, G.; Liashenko, A.; Piskorz, P.; Komaromi, I.; Gomperts, R.; Martin, R. L.; Fox, D. J.; Keith, T.; Al-Laham, M. A.; Peng, C. Y.; Nanayakkara, A.; Gonzalez, C.; Challacombe, M.; Gill, P. M. W.; Johnson, B.; Chen, W.; Wong, M. W.; Andres, J. L.; Gonzalez, C.; Head-Gordon, M.; Replogle, E. S.; Pople, J. A. *GAUSSIAN 98*; Gaussian, Inc.: Pittsburgh, PA, 1998.
- (17) Schaftenaar, V. *MOLDEN*; CAOS/CAMM Center, The Netherlands, 1991.
- (18) (a) Hirschfeld, F. L.; Eriks, K.; Dickerson, R. E.; Lippert, E. L., Jr.; Lipscomb, W. N. *Chem. Phys.* **1958**, *28*, 56. (b) Schwach, D.; Don, B. P.; Burg, A. B.; Beaudet, R. A. *J. Phys. Chem.* **1979**, *83*, 1465. (c) Cheung, C.-C. S.; Beaudet, R. A. *Inorg. Chem.* **1971**, *10*, 1144. (d) Boer, P. F.; Streib, W. E.; Lipscomb, W. N. *Inorg. Chem.* **1964**, *3*, 1666. (e) Pasinski, B. P.; Beaudet, R. A. *J. Chem. Phys.* **1974**, *61*, 683.
- (19) Gunn, S. R.; Green, L. G. *J. Phys. Chem.* **1961**, *65*, 2173.
- (20) The B-H_b-B energy of ca. -0.03 au can be estimated from the experimental dimerization energy of ca. -0.06 au at 0 K (JANAF tables: Chase, M. W., Jr.; Davies, C. A.; Downey, J. R., Jr.; Frurip, D. J.; MacDonald, R. A.; Syverud, A. N. *J. Phys. Chem. Ref. Data* **1985**, *14*, Suppl. 1). One B-H_b-B and one B-B bond are replaced with one B-C bond in carborane, which gives the stabilization energy of ca. -0.03 au.
- (21) Marynick, D. S.; Lipscomb, W. N. *J. Am. Chem. Soc.* **1972**, *94*, 8699.
- (22) Hoffmann, R.; Lipscomb, J. *Chem. Phys.* **1962**, *36*, 2179.